# Density Functional Theory Study of Uranium(VI) Aquo Chloro Complexes in Aqueous Solution

**Michael Bühl,*,# Nicolas Sieffert,‡ Volodymyr Golubnychiy,# and Georges Wipff‡**

*Max-Planck-Institut für Kohlenforschung, Kaiser-Wilhelm-Platz 1, D-45470 Mülheim an der Ruhr, Germany, and UMR 7177 CNRS, Laboratoire MSM, Institut de Chimie, 4 rue Blaise Pascal, 67000 Strasbourg, France*

*Received: October 17, 2007; In Final Form: December 12, 2007*

Mixed uranyl aquo chloro complexes of the type $[UO_2(H_2O)_xCl_y]^{2-y}$ ($y = 1, 2, 3, 4$; $x + y = 4, 5$) have been optimized at the BLYP, BP86, and B3LYP levels of density functional theory in vacuo and in a polarizable continuum modeling bulk water (PCM) and have been studied at the BLYP level with Car−Parrinello molecular dynamics (MD) simulations in the gas phase and in explicit aqueous solution. Free binding energies were evaluated from static PCM data and from pointwise thermodynamic integration involving constrained MD simulations in water. The computations reveal significant solvent effects on geometric and energetic parameters. Based on the comparison of PCM-optimized or MD-averaged uranyl−ligand bond distances with EXAFS-derived values, the transition between five- and four-coordination about uranyl is indicated to occur at a Cl content of $y = 2$ or 3.

## Introduction

The speciation of uranyl(VI) complexes in aqueous solution is of interest for a variety of technological applications. The affinity of the $UO_2^{2+}$ moiety toward anionic complexation partners can be important for processes such as the reprocessing of nuclear waste, where the nitric acid employed[1,2] furnishes a large excess of nitrate ions, or the disposal of nuclear waste in geological salt formations, where concentrated chloride solutions may occur, which can considerably enhance actinide mobility. Stability constants for uranyl mono- and dichloride complexes in aqueous solution have been determined experimentally.[3] Structural information is available for aqueous mono- (**1**), di- (**2**), and trichloride complexes (**3**) from EXAFS studies,[4,5] and for the tetrachloride, $[UO_2Cl_4]^{2-}$ (**4**), from X-ray crystallography.[6] The latter was also ascribed to the species present in a concentrated chloride solution by Dowex anion-exchange resin.[4]

The most recent EXAFS-derived bond distances between uranium and the equatorial ligands are remarkably insensitive to the number of chloro ligands and amount to $U-O^{eq} = 2.41 \pm 0.02$ Å and $U-Cl = 2.71 \pm 0.02$ Å for the complexes with one, two, or three halogens.[5] What appears to be difficult to refine with this technique, however, is the total number of equatorial water and chloro ligands present. Two different fitting models yielded conflicting results, favoring either five-coordination about uranyl, as in the parent uranyl hydrate $[UO_2(H_2O)_5]^{2+}$ (**5**), or four-coordination, as in **4**. Eventually, the former interpretation of the EXAFS data was favored (because the U−Cl distances were noticeably elongated compared to those refined for **4**, which seemed to suggest a higher coordination number), and the species present were formulated as $[UO_2(H_2O)_4Cl]^+$ (**1a**), $[UO_2(H_2O)_3Cl_2]^0$ (**2a**), and $[UO_2(H_2O)_2Cl_3]^-$ (**3a**).[5] In contrast, an earlier EXAFS study had suggested a trend toward lower total coordination numbers with increasing chloride content.[4] It appeared desirable at this point to complement these conflicting findings and interpretations by reliable theoretical calculations for these species.

Quantum-chemical computations of actinide complexes have a long history,[7] as do classical molecular dynamics (MD) simulations with empirical force fields.[8] When these two approaches are bridged, MD simulations are possible on potential energy surfaces derived from density functional theory (DFT), allowing for the explicit inclusion of temperature and solvent effects in the calculations, thereby approaching the actual experimental conditions.[9,10] We have been using DFT-based Car−Parrinello MD (CPMD) simulations in combination with thermodynamic integration to study structures and free energies of uranyl complexes in water. With this methodology, key thermodynamic and kinetic parameters have been successfully reproduced, including the barrier for water exchange[11] and the acidity constant of uranyl hydrate **5**,[12] as well as the binding constant between aqueous uranyl and nitrate.[13] In all these cases, the calculated free energies were found to be within ca. ±2.5 kcal/mol of experiment, a typical accuracy for present-day DFT. We now apply this methodology, as well as conventional static DFT computations, to study uranyl chloro complexes in aqueous solution. Special attention is called to details of the ligand environment about uranyl such as geometrical parameters, coordination number, and stereochemistry. To our knowledge, quantum-chemical computations of uranyl chloro complexes so far have been restricted to **4**[14] and to some uranyl chloro species with an incomplete first solvation shell[15] or to those with acetone instead of water.[16]

## Computational Details

The same methods and basis sets as in our previous studies of uranyl nitrates[10b,c] were employed. Initially, geometries were optimized using the BLYP,[17] BP86,[17a,18] and B3LYP[19,17b] functionals in conjunction with LANL basis, denoting the Los Alamos relativistic effective core potential (ECP) for U together

* Author to whom correspondence should be addressed. Present address: School of Chemistry, North Haugh, University of St. Andrews, St. Andrews, Fife KY16 9ST, U.K. E-mail: buehl@st-andrews.ac.uk.

# Max-Planck-Institut für Kohlenforschung.

‡ Laboratoire MSM.

10.1021/jp710093w CCC: $40.75 
Published on Web 02/13/2008

**CHART 1**

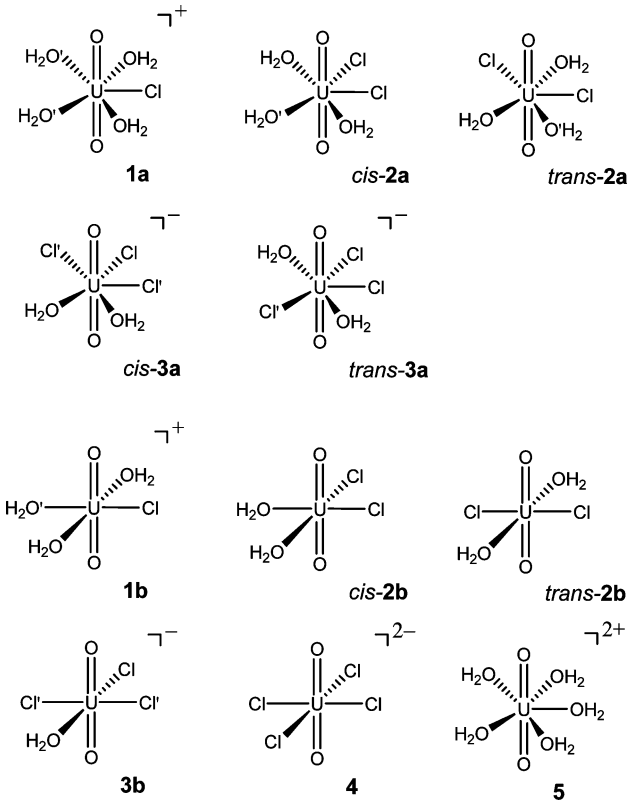


with its (3s3p2d2f) valence basis of contracted Gaussians,[20] standard 6-31G(d,p) basis for all other elements, and a fine integration grid (ultrafine option). The minimum character of each stationary point was verified by computation of the harmonic vibrational frequencies, which were all real. The geometries were reoptimized with the same methods and basis sets using the polarizable continuum model of Tomasi and coworkers[21] (employing the united-atom UFF radii and the parameters of water), denoted PCM. Refined single-point energies for these PCM-optimized geometries were obtained with the same functionals used to optimize the geometry and SDD(+) basis, denoting the small-core Stuttgart−Dresden relativistic ECP together with its valence basis set[22] (from which the most diffuse s-,p-,d-, and f-functions were omitted each, affording a [7s6p5d3f] contraction) and 6-311+G(d,p) basis[23] on all other elements. Results of these computations are summarized in the Supporting Information. Following the suggestion of a referee, all geometries and energies have subsequently been recomputed using the small-core SDD ECP instead of the large-core LANL ECP on U [again using 6-31G-(d,p) basis on the ligands during optimization and 6-311+G-(d,p) for the single points]. These results are given in the main paper and are denoted SDD. Estimates for the basis-set superposition error of individual bonds were computed with the Counterpoise method,[24] employing SDD(+) basis and the PCM/SDD geometries optimized with the respective density functional. These calculations were performed with the Gaussian 03 program.[25]

CP-opt denotes geometries optimized using the CPMD program,[26] until the maximum gradient was less than $5 \times 10^{-4}$ a.u. The BLYP functional was used together with norm-conserving pseudopotentials that had been generated according to the Troullier and Martins procedure[27] and transformed into the Kleinman−Bylander form.[28] For uranium, the semicore (or small-core) pseudopotential was employed that had been generated and validated in ref 10a. Periodic boundary conditions were imposed using cubic supercells with a lattice constant of 13 Å. Kohn−Sham orbitals were expanded in plane waves at the Γ-point up to a kinetic energy cutoff of 80 Ry. For the complexes in vacuo, Car−Parrinello molecular dynamics[29] simulations (denoted CPMD) were performed in the NVT ensemble using a single Nosé−Hoover thermostat set to 300 K (instantaneous heat-up, frequency 1800 $cm^{-1}$), a fictitious electronic mass of 600 a.u., and a time step of 0.121 fs. These unconstrained simulations were followed over 2−4 ps, the first 0.5 ps of which were taken for equilibration.[30] For the aqueous solutions, labeled CPMD(aq), the boxes were filled with 56, 55, and 54 water molecules for **1, 2** and **3**, respectively, affording a density of ca. 1.0 g $cm^{-3}$. In order to maintain the time step, hydrogen was substituted with deuterium, and in order to increase the mobility of the solvent, the thermostat was set to 320 K. Long-range electrostatic interactions were treated with the Ewald method. No electrostatic decoupling between replicated cells was included, as it had been shown that no noticeable errors are introduced by this procedure even for divalent ions.[31] Starting structures were generated from previous well-equilibrated simulations (e.g., uranyl mononitrate from ref 13) by manually replacing the anionic ligand with the appropriate number of chlorine atoms and water molecules.

Constrained CPMD and CPMD(aq) simulations were performed along predefined reaction coordinates (bond distances $r$) connecting complexes with different coordination numbers, in order to evaluate the change in the Helmholtz free energy by pointwise thermodynamic integration (PTI)[32] of the mean constraint force $\langle f \rangle$ along these coordinates via

$$\Delta A_{a \to b} = -\int_a^b \langle f(r) \rangle \mathrm{d}r \qquad (1)$$

At each point, the system was propagated until $\langle f \rangle$ was sufficiently converged (usually within 1.5−2 ps after 0.5 ps of equilibration, similar to the degree of convergence documented in Figure S1 of the Supporting Information for ref 10a). Each new point was continued from the final, equilibrated configuration of the previous one, using 2000 steps of continuous slow growth to increase the constrained distance.

## Results

The molecules of this study are sketched in Chart 1. In the first part of this section, structural parameters of these complexes are discussed, whereas the second part will concentrate on salient energetics.

**1. Geometries.** Optimized geometrical parameters of **1**−**5** are collected in Table 1, together with experimental data, where available. All isomers are characterized as minima in the gas phase at the DFT/SDD levels. In most cases, these minima have $C_1$ symmetry, due to intramolecular interactions between one or more of the positively charged H atoms and coordinated electronegative O or Cl atoms. In the MD simulations in the gas phase, however, rotations of bound water ligands about the U−O bonds are frequently observed, which essentially make those bonds equivalent that bear the same label in Chart 1 (primed or unprimed). We thus report the correspondingly averaged values also for the static minima in the gas phase. The DFT/SDD minima were also reoptimized in a polarizable continuum (labeled PCM in Table 1); here, several of the stationary points that were located do not correspond to true minima but rather to transition states for rotations of one or more water ligands. Because these rotations are associated with fairly low imaginary frequencies below $20i$ $cm^{-1}$,[33] and because

**TABLE 1: Geometrical Parameters (Bond Distances in Å)[a] of Complexes 1−5, Computed with the BLYP Functional [in Square Brackets: B3LYP/SDD] and Refined from EXAFS Data in Solution**

| compd | bond | gas SDD | PCM SDD | gas B3LYP | PCM B3LYP | CP-opt | CPMD | $CPMD_{aq}$ | exp[b] | exp[c] |
|---|---|---|---|---|---|---|---|---|---|---|
| **1a** | *r*(U═O) | 1.80 | 1.81 | [1.76] | [1.77] | 1.79 | 1.80(2) | 1.82(2) | 1.76 | 1.76 |
| | *r*(U−Cl) | 2.61 | 2.69 | [2.59] | [2.69] | 2.61 | 2.61(6) | 2.76(9) | 2.71 | 2.71 |
| | *r*(U−O) | 2.58 | 2.48 | [2.55] | [2.46] | 2.55 | 2.60(11) | 2.48(9) | 2.41 | 2.41 |
| | *r*(U−O′) | 2.55 | 2.52 | [2.54] | [2.49] | 2.57 | 2.64(11) | 2.49(9) | | |
| **1b** | *r*(U═O) | 1.80 | 1.81 | [1.76] | [1.77] | 1.80 | 1.80(1) | 1.82(3) | | |
| | *r*(U−Cl) | 2.56 | 2.64 | [2.54] | [2.64] | 2.55 | 2.56(6) | 1.68(6) | | |
| | *r*(U−O) | 2.48 | 2.40 | [2.47] | [2.39] | 2.48 | 2.52(8) | 2.38(6) | | |
| | *r*(U−O′) | 2.50 | 2.40 | [2.49] | [2.40] | 2.52 | 2.57(7) | 2.39(7) | | |
| *cis*-**2a** | *r*(U═O) | 1.81 | 1.81 | [1.77] | [1.77] | 1.80 | →*cis*-**2b**·$H_2O$ | − | | |
| | *r*(U−Cl) | 2.66 | 2.72 | [2.65] | [2.71] | 2.65 | →*cis*-**2b**·$H_2O$ | − | | |
| | *r*(U−O) | 2.68 | 2.54 | [2.64] | [2.51] | 2.72 | →*cis*-**2b**·$H_2O$ | − | | |
| | *r*(U−O′) | 2.63 | 2.58 | [2.60] | [2.54] | 2.66 | →*cis*-**2b**·$H_2O$ | − | | |
| *cis*-**2b** | *r*(U═O) | 1.81 | 1.81 | [1.77] | [1.77] | 1.81 | 1.81(2) | − | | |
| | *r*(U−Cl) | 2.62 | 2.67 | [2.60] | [2.66] | 2.61 | 2.61(5) | − | | |
| | *r*(U−O) | 2.56 | 2.43 | [2.54] | [2.41] | 2.57 | 2.66(12) | − | | |
| trans-**2a** | *r*(U═O) | 1.80 | 1.81 | [1.77] | [1.78] | 1.80 | →trans-**2b**·$H_2O$ | 1.82(2) | 1.76 | 1.76 |
| | *r*(U−Cl) | 2.71 | 2.74 | [2.70] | [2.73] | 2.70 | →trans-**2b**·$H_2O$ | 2.77(10) | 2.71 | 2.73 |
| | *r*(U−O) | 2.55 | 2.51 | [2.52] | [2.49] | 2.55 | →trans-**2b**·$H_2O$ | 2.46(8) | 2.41 | 2.50 |
| | *r*(U−O′) | 2.60 | 2.54 | [2.57] | [2.51] | 2.62 | →trans-**2b**·$H_2O$ | 2.53(10) | 2.41 | 2.50 |
| trans-**2b** | *r*(U═O) | 1.81 | 1.81 | [1.77] | [1.77] | 1.81 | 1.80(2) | 1.81(3) | 1.76 | 1.76 |
| | *r*(U−Cl) | 2.64 | 2.68 | [2.63] | [2.68] | 2.63 | 2.65(7) | 2.73(8) | 2.71 | 2.73 |
| | *r*(U−O) | 2.53 | 2.43 | [2.51] | [2.40] | 2.52 | 2.59(11) | 2.38(7) | 2.41 | 2.50 |
| *cis*-**3a** | *r*(U═O) | 1.82 | 1.82 | [1.78] | [1.78] | 1.81 | →**3b**·$H_2O$ | − | | |
| | *r*(U−Cl) | 2.64 | 2.74 | [2.63] | [2.72] | 2.64 | →**3b**·$H_2O$ | − | | |
| | *r*(U−Cl′) | 2.81 | 2.78 | [2.80] | [2.77] | 2.80 | →**3b**·$H_2O$ | − | | |
| | *r*(U−O) | 2.72 | 2.60 | [2.69] | [2.56] | 2.76 | →**3b**·$H_2O$ | − | | |
| trans-**3a** | *r*(U═O) | →*cis*-**2b**·$Cl^-$ | 1.81 | [1.77] | [1.78] | 1.81 | →*cis*-**2b**·$Cl^-$ | →**3b**·$H_2O$ | | |
| | *r*(U−Cl) | →*cis*-**2b**·$Cl^-$ | 2.76 | [2.69] | [2.75] | 2.64 | →*cis*-**2b**·$Cl^-$ | →**3b**·$H_2O$ | | |
| | *r*(U−Cl′) | →*cis*-**2b**·$Cl^-$ | 2.80 | [2.97] | [2.79] | 2.80 | →*cis*-**2b**·$Cl^-$ | →**3b**·$H_2O$ | | |
| | *r*(U−O) | →*cis*-**2b**·$Cl^-$ | 2.57 | [2.60] | [2.54] | 2.76 | →*cis*-**2b**·$Cl^-$ | →**3b**·$H_2O$ | | |
| **3b** | *r*(U═O) | 1.81 | 1.82 | [1.77] | [1.78] | 1.81 | 1.81(2) | 1.82(3) | 1.76 | 1.77 |
| | *r*(U−Cl) | 2.66 | 2.69 | [2.64] | [2.68] | 2.65 | 2.65(4) | 2.69(6) | 2.71 | 2.73 |
| | *r*(U−Cl′) | 2.73 | 2.71 | [2.71] | [2.70] | 2.71 | 2.72(8) | 2.74(9) | | |
| | *r*(U−O) | 2.65 | 2.44 | [2.62] | [2.42] | 2.69 | 2.73(12) | 2.41(7) | 2.41 | 2.52 |
| **4** | *r*(U═O) | 1.82 | 1.82 | [1.78] | [1.78] | 1.82[c] | 1.82(2)[d] | 1.82(4)[d] | | 1.76 |
| | *r*(U−Cl) | 2.77 | 2.73 | [2.75] | [2.72] | 2.72[c] | 2.76(8)[d] | 2.71(8)[d] | | 2.67 |
| **5** | *r*(U═O) | 1.78 | 1.80 | [1.75] | [1.76] | 1.78[c] | 1.78(1)[d] | 1.81(3)[d] | 1.76 | 1.77 |
| | *r*(U−O) | 2.50 | 2.46 | [2.49] | [2.44] | 2.50[c] | 2.54(8)[d] | 2.48(10)[d] | 2.41 | 2.42 |

[a] Averaged values, where appropriate; in parentheses: standard deviations over the CPMD trajectories (last 2−2.5 ps); see Chart 1 for definition. [b] EXAFS data from ref 5 (quoted uncertainties ± 0.02 Å). [c] EXAFS data from ref 4 (quoted uncertainties ± 0.02 Å), using the numbers obtained at chloride concentrations of 4, 10, and 16 M for **1**, **2**, and **3**, respectively. [d] Box length 11.5 Å, from ref 10.

there are typically quite large amplitudes for such rotations in the CPMD simulations in water (albeit without showing free rotation on the short time scales that could be followed), the geometrical parameters (and in particular, the total energies) of these saddle points should be reasonably good approximations to those of the actual PCM minima. We thus did not attempt to locate the latter in all cases. The initial LANL optimizations were effected with several exchange correlation functionals. The BP86/LANL optimized distances were found to be consistently shorter by ca. 0.01− 0.03 Å than those at the BLYP/LANL level. In context with the CPMD simulations in water, we will discuss preferentially the BLYP/SDD values, because that functional performs better for describing the properties of liquid water.[34] The LANL data are given as Supporting Information. Because hybrid functionals can be superior to pure GGAs for certain thermodynamic properties,[35,36] we have also performed B3LYP/SDD optimizations (values in square brackets in Table 1).

We will first turn to the static optimized geometries in the gas phase. On going from the BLYP to the B3LYP functional, the bond lengths tend to shrink by ca. 0.01−0.04 Å (compare SDD and [B3LYP] entries in Table 1), consistent with previous experience with first- and second row transition-metal complexes.[37] In particular, the distances to the terminal oxo ligands, labeled *r*(U═O), are quite sensitive to the functional.[38] By and large, the BLYP/SDD and BLYP/CP-opt derived distances are quite close to each other. With the large-core LANL ECP on uranium (instead of the small-core SDD variant), some U−Cl bond lengths are overestimated significantly, by ca. 0.05−0.1 Å (see Table S1 in the Supporting Information). The shortcomings of the large-core LANL ECP had been noted before in context with computed thermodynamic properties.[39]

Among the five-coordinated complexes, only **1a** is stable (or at least metastable) for a few picoseconds in unconstrained CPMD simulations in the gas phase. All others spontaneously rearrange to four-coordinated species with an additional ligand in the second coordination sphere (indicated by the arrows in Table 1). For *cis*- and *trans*-**2a**, as well as *cis*-**3a**, a water ligand detaches, whereas for *trans*-**3a** it is a chloride ligand (Cl′ in Chart 1) that is expelled, affording a complex between *cis*-**2b** and $Cl^-$, which is stabilized by two strong hydrogen bonds between the chloride and two OH moieties from the adjacent water ligands. The latter transition occurs already during geometry optimization with the LANL ECP, both with BLYP and B3LYP functionals, indicative of a rather weak affinity of **2b** for a third chloro ligand (see below). On going from the equilibrium geometry to the dynamic average in vacuo, all bond lengths increase, as expected for anharmonic stretching poten-

**TABLE 2: Computed Energies and Free Energies (in Kcal/mol) for the Cumulated Chloride Binding Energies of Uranyl Hydrate According to Eq 4 (SDD Level)**

| | BLYP | | | | B3LYP | | | |
|---|---|---|---|---|---|---|---|---|
| *n* | Δ (gas) | Δ*E* PCM | Δ*G* PCM | Δ*E* [Δ*E*$^{CP}$] SDD(+)/PCM[a] | Δ*E* (gas) | Δ*E* PCM | Δ*G* PCM | Δ*E* [Δ*E*$^{CP}$] SDD(+)/PCM[a] |
| 1 | −202.0 | −4.5 | −6.5 | −8.4 [−9.5] | −197.8 | −2.8 | −4.4 | −6.0 [−7.2] |
| 2 (cis) | −321.2 | −5.6 | −10.0 | −13.7 [−15.9] | −314.6 | −2.8 | −6.1 | −9.3 [−11.6] |
| 2 (trans) | −324.4 | −5.7 | −9.7 | −13.7 [−15.9] | −319.3 | −3.3 | −6.7 | −9.9 [−11.9] |
| 3 (cis) | −361.2 | −2.9 | −10.6 | −15.2 [−18.3] | −353.4 | 0.3 | −6.0 | −10.0 [−11.5] |
| 3 (trans) | −368.1[b] | −3.5 | −10.5 | −15.9 [−18.9] | −356.2[b] | −0.8 | −6.8 | −11.1 [−12.6] |
| 4 | (−326.0) [c] | 4.0 | −6.7 | −13.2 [−17.6] | (−319.8)[c] | 7.2 | −1.5 | −7.3 [−12.0] |

[a] Single point energies using 6-311+G(d,b) basis on the ligands [in square brackets: counterpoise-corrected energies (see ref 41)]. [b] *trans*-**3a** optimized to *cis*-**2b**·$Cl^-$ in the gas phase. [c] Because no $[UO_2(H_2O)Cl_4]^{2-}$ minimum can be located in the gas phase, these values in parentheses refer to a microsolvated $[UO_2Cl_4]^{2-}\cdot(H_2O)$ complex; all other entries in this row are for the five-coordinate $[UO_2(H_2O)Cl_4]^{2-}$ species that can be optimized in the continuum.

tials (compare CP-opt and CPMD values in Table 1). In general the U−Cl bonds are less strongly affected than the U−O bonds to the water ligands, which tend to increase by ca. 0.05−0.09 Å upon dynamic averaging. As more and more water ligands are replaced with the bulkier chloride ions, all bond distances in the four-coordinate complexes increase; e.g. on going from **1b** to **3b**, the CPMD-derived mean U−Cl distance increases from 2.56 to 2.70 Å (U−O from 2.55 to 2.73 Å).

Selected complexes were subsequently studied with CPMD in aqueous solution. As the static cis and trans isomers of a given complex turned out to be very similar in energy (see below), only one of both isomers was explicitly simulated for each of **2** and **3**, namely, the corresponding trans forms. Five-coordinated **1a** and *trans*-**2a** remained stable in the unconstrained MD runs in water, whereas *trans*-**3a** rapidly (after 1.8 ps) lost one water ligand to the bulk, affording aqueous **3b**. This outcome is in interesting contrast to that of the simulation in the gas phase (which started from the same five-coordinate *trans*-**3a** configuration), where a chloride ion was expelled during the MD.

For all complexes where a direct comparison between CPMD in vacuo and in water is possible, solvation significantly reduces the U−O bond distances to the coordinated water ligands, by up to 0.21 Å. There is a trend toward a concomitant increase in the U−Cl distances, which is most pronounced in cationic **1a** (increase by 0.15 Å), attenuated in neutral *trans*-**2b** (increase by 0.08 Å), and all but disappeared in monoanionic **3b** (small net increase of 0.02 Å in the mean distances). A similar differential solvation effect on neutral and anionic ligands had been noted previously for uranyl nitrate complexes.[10b,c] For dianionic **4**, hydration produces a significant reduction of the U−Cl distance, by 0.05 Å. It is noteworthy that all these trends are reproduced qualitatively in static optimizations employing a polarizable continuum, irrespective of the functional (compare SDD and PCM/SDD, or B3LYP and PCM/B3LYP values in Table 1).

For five-coordinate **1a**, the CPMD(aq) distances agree reasonably well with the EXAFS data, showing the typical (see above) overestimation of the bond lengths.[40] The simulated U−Cl and mean U−O distances are overestimated by ca. 0.05 Å and 0.08 Å, respectively, similar to the degree of agreement for **4** and **5** (note that these deviations would likely be reduced with hybrid functionals). Assessment of the geometrical parameters for di- and trichlorides are best made in terms of relative changes from the monochloride. Experimentally, these changes are indicated to be undetectably small, which has been taken as indication of constant coordination number. On going from **1a** to five-coordinated *trans*-**2a**, both U−Cl and mean U−O distances expand slightly, by 0.01 and 0.02 Å, respectively, at the CPMD(aq) level, similar to what is found in the static PCM computations, e.g., 0.04 and 0.02 Å, respectively, at the PCM/B3LYP level. The latter predicts a further considerable increase when the Cl content is increased at constant coordination number, amounting to a total change of U−Cl and mean U−O distances by 0.08 and 0.07 Å, respectively, between **1a** and *trans*-**3a**. In particular the computed change in the U−Cl distance appears large enough to be detectable. In contrast, on going from five-coordinated **1a** to four-coordinated higher chlorinated species entails much smaller changes: for example, for the change of the mean U−Cl distance between **1a** and **3b**, the PCM/B3LYP and CPMD(aq) levels predict 0.0 Å and −0.04 Å, respectively, which would seem more compatible with experiment.

To summarize this section, the computed bond distances between uranyl and chloro or water ligands are sensitive to the computational model (ECP, density functional), thermal averaging, and solvation. For the five-coordinate monochloride **1a** modeled in water (either explicitly or with a continuum), simulated and refined parameters agree reasonably well, within the accuracy found for other uranyl complexes so far. All computational models agree that there is a tendency to increase all metal−ligand distances as water ligands are replaced by chloride ions at constant coordination number, and to decrease these distances as the coordination number is reduced from five to four by removing a water ligand.

**2. Relative Energies.** The coordination number about uranyl depends on the affinities toward the different ligands, water and chloride in our case. We will first turn to the binding energies of chloride ions, because the first two binding constants in water are known experimentally,[3] from which free energies can be derived for the following processes:

$$UO_2^{2+} + Cl^- \rightleftharpoons UO_2Cl^+,\ \Delta G^0 = -0.2\ \text{kcal/mol} \quad (2)$$

$$UO_2^{2+} + 2Cl^- \rightleftharpoons UO_2Cl_2,\ \Delta G^0 = +1.5\ \text{kcal/mol} \quad (3)$$

It should be noted that the actual equilibrium constants depend noticeably on the ionic strength of the solution[3c] (see below). Table 2 summarizes some salient energetic data computed at various DFT levels involving static PCM optimizations and single-point energy evaluations for the following processes:

$$[UO_2(H_2O)_5]^{2+} + n Cl^- \rightleftharpoons [UO_2(H_2O)_{5-n}Cl_n]^{2-n} + n H_2O \quad (4)$$

**TABLE 3: Computed Energies and Free Energies (in kcal/mol) for Water Dissociation from Uranyl Aquo Chloro Complexes According to Eq 7**

| | BLYP | | | | B3LYP | | | |
|---|---|---|---|---|---|---|---|---|
| *n* | $\Delta E$ (gas) | $\Delta E$ PCM | $\Delta G^d$ PCM | $\Delta E$ [$\Delta E^{CP}$] SDD(+)/PCM[a] | $\Delta E$ (gas) | $\Delta E$ PCM | $\Delta G^d$ PCM | $\Delta E$ [$\Delta E^{CP}$] SDD(+)/PCM[a] |
| 0 | 28.6 | 19.1 | 9.9 | 9.6 [7.6] | 30.0 | 19.9 | 12.5 | 12.1 [10.1] |
| 1 | 20.8 | 15.1 | 6.2 | 6.1 [4.1] | 22.2 | 16.0 | 7.5 | 8.6 [6.6] |
| 2 (cis) | 16.9 | 11.2 | 2.0 | 3.2 [1.2] | 17.7 | 12.3 | 4.6 | 5.6 [3.6] |
| 2 (trans) | 20.5 | 12.2 | 3.7 | 4.4 [2.4] | 23.7 | 13.3 | 4.8 | 6.4 [4.4] |
| 3 (cis) | 10.9 | 7.4 | -1.0 | -0.1 [-2.1] | 10.0 | 8.3 | 0.7 | 2.3 [1.3] |
| 3 (trans) | 17.8[b] | 7.9 | −1.1 | 0.6 [−1.4] | 12.8[b] | 9.3 | 1.5 | 3.3 [1.3] |
| 4 | (16.5)[c] | 1.5 | −6.1 | −4.8 [−6.8] | (16.9)[c] | 2.5 | −5.0 | −2.6 [−4.6] |

[a−c] See corresponding footnotes in Table 2. [d] Entropies evaluated at a pressure of 1345 atm (see text).

Computation of these data is straightforward, but simplistic, because the models involve many approximations such as that of a simple continuum without specific hydrogen bonds, or that of an ideal-gas behavior for derivation of the thermodynamic functions. Furthermore, significant BSSE[41] and only little favorable error cancelation is to be expected. The PCM results correctly reproduce the qualitative finding that the binding energies between uranyl and chlorides are much smaller in water than in the gas phase, where oppositely charged ions always attract each other strongly. Quantitatively, however, the binding strengths still appear to be overestimated in water. For instance, for the equation

$$[UO_2(H_2O)_5]^{2+}\ (\mathbf{5}) + Cl^- \rightleftharpoons [UO_2(H_2O)_4Cl]^+\ (\mathbf{1a}) + H_2O \quad (2a)$$

the equivalent of eq 2 assuming five-coordination about uranyl throughout, driving forces of $\Delta G = -6.5$ to $-4.4$ kcal/mol are computed, depending on the functionals (see $\Delta G$ entries for $n = 1$ in Table 2), i.e., significantly more negative than the observed value, $-0.2$ kcal/mol. What is more, binding of two or more chloride ions is computed to be even more favorable than that of one, in qualitative disagreement with experiment. Increasing the basis set does not appear to improve the PCM results (compare $\Delta E$ PCM and $\Delta E$ SDD(+)/PCM entries in Table 2). We note in passing that corresponding cis or trans isomers are predicted to be very close in energy at all levels, well within 1 kcal/mol in most cases. It has been proposed to model reactions of type 4 as an intramolecular exchange between molecules from the first and second coordination sphere in suitable outer-sphere complexes.[42] While this approach might be feasible for the single exchange in reaction 2a, it would be rather cumbersome for larger chloride numbers *n* because of the very many possible minima that have to be considered for such microsolvated clusters.

Deriving free energies in the dynamic ensemble of explicitly solvated complexes is a way to go beyond the simple static PCM picture. We have done this by means of constrained CPMD simulations along two consecutive paths designed to mimic the process in eq 2a. In analogy to our study on the binding free energies between uranyl and nitrate or pertechnetate,[13] we have first constructed a path for dissociation of the anionic ligand according to

$$[UO_2(H_2O)_4Cl]^+\ (\mathbf{1a}) \rightarrow [UO_2(H_2O)_4]^{2+} + Cl^- \quad (5)$$

and evaluated the free energy for this process[43] via thermodynamic integration, using the U−Cl distance *r* as reaction coordinate. The resulting free-energy profile is depicted in Figure 1 (lower, solid curve). Starting from the minimum **1a** at $r = 2.76$ Å, the contact ion pair is reached at $r \approx 4.6$ Å, at which point the mean constraint force is essentially zero. This point is higher in free energy than the starting point by $\Delta A = 5.4$ kcal/mol, with a barrier of $\Delta A^{\ddagger} = 9.1$ kcal/mol at $r \approx 3.8$ Å, with a numerical uncertainty of ca. ±0.8 kcal/mol. As in our previous PTI studies,[10−12] the uncertainty was estimated from the largest standard deviation of the running average of $\langle f \rangle$ during the last ps of the constrained runs, multiplied with the total integration width.[44]

Complete dissociation of the ion pair depicted in the lower right of Figure 1 into the infinitely separated constituents (which would correspond to the ideal state of infinite dilution) is, evidently, impractical to model with this approach. According to a simple estimate from the literature, the free energy necessary to separate such a contact ion pair (or outer-sphere complex) formed between a dication and a monoanion should amount to +1 kcal/mol.[45] The free binding energy of a water ligand in uranyl pentahydrate **5**, according to

$$[UO_2(H_2O)_5]^{2+} \rightarrow [UO_2(H_2O)_4]^{2+} + H_2O \quad (6)$$

had been simulated with the same methodology to be $\Delta A = +8.7$ kcal/mol.[10a] Thus, the total driving force for chloride binding according to eq 2a (including the estimate for ion-pair dissociation) is computed to be $\Delta A = 8.7 - (5.4 + 1.0) = +2.3$ kcal/mol at the CPMD(aq) level.[46] Even though this number has the wrong sign compared to experiment ($\Delta G^0 = -0.2$ kcal/mol), it does constitute an improvement over the static BLYP/PCM results in Table 2 and falls just within the accuracy of ±2.5 kcal/mol established so far for the thermodynamic and kinetic properties of aqueous uranyl complexes computed with this CPMD-based approach. It should be noted that the situation modeled in the CPMD simulation does not correspond to the ideal standard state of infinite dilution. With a roughly 1 M concentration (and a corresponding ionic strength), equilibrium constants can be inferred from the experimental data that would correspond to small and positive $\Delta G$ values on the order of +0.5 kcal/mol (see Table 9.3 and example 2 on p 341ff. in ref 3c), which would improve the accord between simulation and experiment.

In order to assess the effect of the solvent, we have followed the dissociation path of eq 5 also in the gas phase. The resulting free-energy profile is included in Figure 1 (upper, dotted curve). At $r = 3.6$ Å, a spontaneous proton transfer occurred, affording a $[UO_2(H_2O)_3(OH)]^+ \cdot HCl$ complex. In order to prolong the path further, we have imposed two additional constraints from this point on, namely fixing the two OH distances that form the hydrogen bridge to the leaving chloride (see the snapshot in the upper right of Figure 1) to their mean values at the point with $r = 3.4$ Å. Because significant mean forces are accumulated

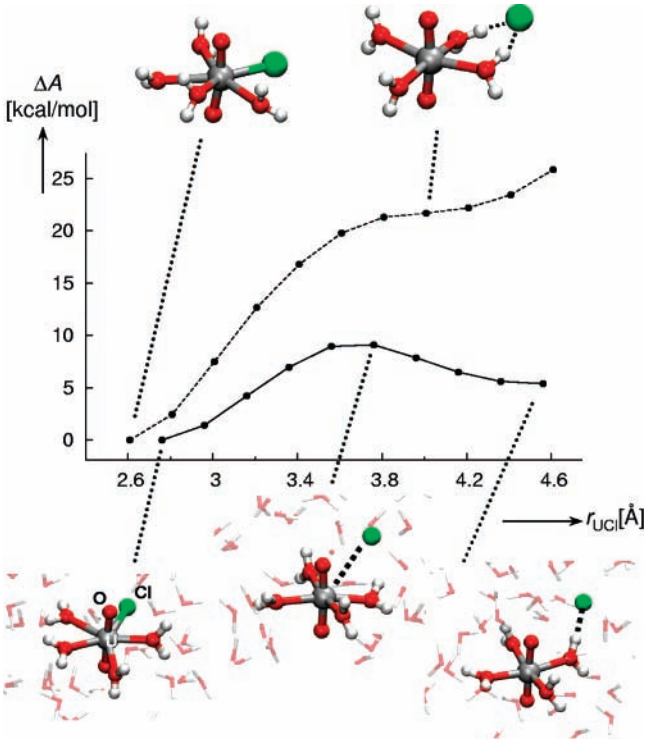


**Figure 1.** Change in free energy, $\Delta A$, for dissociation of the chloride ligand in $[UO_2(H_2O)_4Cl]^+$ (**1a**), as obtained from constrained CPMD simulations and thermodynamic integration, including representative snapshots from the indicated regions (reaction coordinate: U−Cl distance). Top: gas phase (dashed line); bottom: aqueous solution (solid line).

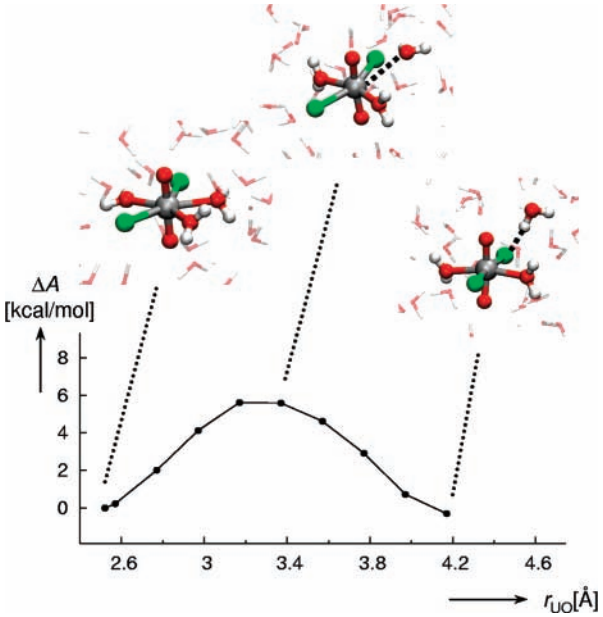


**Figure 2.** Change in free energy, $\Delta A$, for dissociation of one water ligand in aqueous *trans*-$UO_2(H_2O)_3Cl_2$ (*trans*-**2a**), as obtained from constrained CPMD simulations and thermodynamic integration, including representative snapshots from the indicated regions (reaction coordinate: U−O distance).

on these additional constraints as $r$ is increased, the calculated $\Delta A$ values from this point onward are probably only to be used as a rough guide. Interestingly, a plateau is reached in the free-energy profile at $r = 4.0$ Å, characterized by a near-zero mean constraint force on $r$, which is 21.7 kcal/mol above **1a**. Starting from the last snapshot of this point, we can optimize a stationary point on the potential energy surface (with a fully optimized U−Cl distance of $r = 4.02$ Å at the CP-opt level), which is 14.9 kcal/mol above the fully optimized minimum **1a**. For larger values of $r$ beyond this apparent plateau, the simulated free energy continues to rise, and would, in the limit of an infinitely large box, eventually attain a value on the order of 200 kcal/mol (cf. the gas-phase energies in Table 2 for $n = 1$). We note that at that point where the chloride atom has completely left the coordination sphere of uranyl in water ($r \approx 4.6$ Å), the stabilization of the contact ion pair due to hydration amounts to ca. 20 kcal/mol, as judged by the difference in $\Delta A$ between the two curves in Figure 1 at that point.

We now turn to the question of the total coordination number about uranyl for a given number of chloro ligands. This question is assessed by computing the water binding energies according to the following dissociation reactions:

$$[UO_2(H_2O)_{5-n}Cl_n]^{2-n} \rightleftharpoons [UO_2(H_2O)_{4-n}Cl_n]^{2-n} + H_2O \quad (7)$$

The results are summarized in Table 3. The absolute raw binding energies $\Delta E$ are certainly overestimated, because of basis-set superposition error.[41] In order to model the changes in entropy for the condensed phase, reflected in the changes between corresponding $\Delta E$ and $\Delta G$ values, the standard expressions from statistical thermodynamics have been evaluated at a pressure of 1345 atm.[47] Because of the crude nature of the basic assumptions, the simple continuum model for solvation energies and the ideal-gas model for enthalpic and entropic contributions in solution, only qualitative conclusions can be made based on these static results: As expected, the propensity for five-coordination drops significantly with increasing chlorine content. While all levels agree that the monochloride **1** should be five-coordinated (as all $\Delta E$ and $\Delta G$ values in the second row of Table 3 are positive), the trichloride is indicated to prefer four-coordination in water (cf. the negative or very small $\Delta G$ and $\Delta E$ SDD(+)/PCM values in the fifth and sixth rows), in accordance with the results of the unconstrained CPMD simulations of aqueous **1a** and *trans*-**3a** discussed in the preceding section.

The dichloride may just be borderline. In order to go beyond the static PCM picture in this case, we studied water dissociation from *trans*-**2a** in aqueous solution by constrained CPMD and thermodynamic integration. During the unconstrained simulation of this complex (which are documented in Table 1), one of the water ligands turned out to be somewhat more labile than the others, as it reached longer instantaneous U−O distances during the fluctuations along the trajectory. The $r$(U−O) distance to this ligand was therefore chosen as constraint for a reaction coordinate and was subsequently elongated stepwise by 0.2 Å, affording the free-energy profile shown in Figure 2.

After passing a barrier of $\Delta A^{\ddagger} = 5.6$ kcal/mol at $r = 3.2$ Å, the product, *trans*-**2b**, is obtained at $r = 4.2$ Å and $\Delta A = -0.7$ kcal/mol, with an estimated numerical uncertainty of $\pm 0.7$ kcal/mol.[44] Thus, the CPMD simulations (which are free of BSSE and should account reasonably well for entropic effects) also predict a very weak binding of the fifth water ligand. Five- and four-coordinated **2a** and **2b** are indicated to be essentially isoenergetic in water at the BLYP level and would thus be present in form of an equilibrium mixture. Given the increase of the water dissociation energy on going from the static BLYP to B3LYP levels (by ca. 2.5 kcal/mol, compare, for example, the corresponding $\Delta E$ SDD(+)/PCM entries for $n = 2$ in Table 3), a slight preference for five-coordination should persist at

the B3LYP level, which would suggest **2a** to be the major component of such a mixture. As mentioned above, four-coordinate species **3b** is likely to be more prominent for the trichloride, also at the B3LYP level.

## Discussion and Concluding Remarks

Elucidating the precise coordination environment about uranyl in mixed aquo chloro complexes in aqueous solution is a difficult task both for experimental and computational techniques. With oxygen donors, the overwhelming majority of uranyl(VI) complexes prefers five-coordination in the equatorial plane,[48,49] with the pentahydrate **5** as the archetypical example. In contrast, when four chloro ligands are present, it appears difficult to increase the coordination number beyond four.[6,50] The transition between preferential five- and four-coordination must occur at an intermediate chlorine content. All DFT-based methods applied in this study agree that the monochloride complex **1** should be five-coordinated and should therefore be formulated as $[UO_2(H_2O)_4Cl]^+$ (**1a**). This assignment is supported by the good agreement (at least within the accuracy typically achievable for a particular density functional) of the PCM-optimized or CPMD(aq)-simulated bond distances with those derived from EXAFS spectroscopy (Table 1). For the four-coordinate variant **1b**, the optimized or CPMD(aq)-derived U−O distances involving the water ligands are slightly shorter than the experimental estimates, which would be very uncommon for this level of DFT. We have not computed the free energy of water dissociation from **1a** explicitly with constrained CPMD simulations and thermodynamic integration. The corresponding $\Delta A$ value for monocationic **1a** is expected to fall within those simulated with this approach for dicationic **5**, +8.7 kcal/mol,[10a] and neutral *trans*-**2a**, −0.7 kcal/mol (Figure 2), probably closer to the former than to the latter (cf. the corresponding PCM data for $n = 0-3$ in Table 3). The assignment of the aqueous monochloro complex to five-coordinate **1a** can thus be made with some confidence.

Already for the dichloride **2**, static BLYP and B3LYP optimizations, as well as dynamic BLYP simulations predict a very weak binding of one water ligand or an actual preference of four- over five-coordination in water. This preference is somewhat less pronounced with the B3LYP than with the BLYP functional, or with an explicit solvation model than in a simple polarizable continuum (compare the numbers in Table 3 for $n = 2$ with the CPMD-derived $\Delta A = -0.7$ kcal/mol for water dissociation in *trans*-**2a**, Figure 2). No clear distinction between **2a** and **2b** can be made based on these results. Given the propensity of DFT to underestimate binding energies of water ligands in transition-metal or uranyl complexes,[51,52] it is well possible that five-coordination may actually prevail in the dichloro complex.

All DFT methods applied in this study agree that the preference for four- over five-coordination should be more pronounced for the trichloride **3** than for **2** (see entries for $n = 2$ and 3 in Table 3). Five-coordinate variants of **3a** can only be located as stationary points on potential energy surfaces but are indicated to be unstable in CPMD simulations, both in vacuo and in water (at least with the BLYP functional). Given that for **1a** and **2a**, the PCM-optimized distances (in particular with the B3LYP functional) are in good accord with the CPMD(aq) values and the EXAFS estimates (Table 1), the PCM/B3LYP predictions for **3a** should also be reliable. Because at that level, the uranyl−ligand distances are significantly elongated with respect to those in **1a** (Table 1); there would be a considerable deterioration in comparison with the newer EXAFS values, which are essentially invariant between **1** and **3**. PCM-optimized and CPMD(aq)-simulated geometrical parameters of four-coordinate **3b**, on the other hand, are not very disparate from those of five-coordinate **1a** and, thus, from the EXAFS values (Table 1). Taken together, the structural and energetic results presented herein strongly suggest that the uranyl trichloro complex can accommodate only one additional water ligand in solution and that it should thus be formulated as four-coordinate **3b** (perhaps as the principal component of an equilibrium mixture with **3a**).[53] If real, the apparent insensitivity of the U−O and U−Cl distances toward the chlorine content between **1** and **3**, as suggested by the newer EXAFS analysis,[5] is indicated to arise from a balance between the tendencies to increase these distances with the chlorine content at constant coordination number and to decrease them upon removal of one water ligand. By and large, our results serve to support the earlier interpretation of the EXAFS data,[4] according to which the total coordination number about uranyl decreases with increasing chloride loading. Specifically, on going from the refined number of chloro ligands $n = 1.0$ to $n = 2.6$ (the highest value at 14 M chloride concentration), the total coordination number has been reported to drop from 4.9 to 4.5. Even though this change is not significant with a quoted uncertainty in the respective atom numbers of $\pm 0.3$,[4] this result would be compatible with our predicted change in coordination number when $n$ becomes larger than 2.

Where di- and tri-chlorides can exist as different stereoisomers (labeled cis and trans in this study, see Chart 1), the PCM-based results predict little energetic discrimination between them. In no case do relative energies or free energies between cis and trans isomers (which can be inferred from the reaction energies in Table 2) exceed 1.1 kcal/mol. For instance, four-coordinate *cis*- and *trans*-**2b** are computed to be within 0.0−0.6 kcal/mol of each other at the SDD(+)/PCM level (with BLYP and B3LYP, respectively). This result is in qualitative accord with observations that cis and trans isomers of phosphinoxide complexes $UO_2Cl_2(OPCy_3)_2$ can coexist in $CH_2Cl_2$ solution (the related phosphinimine derivatives even in the solid).[54] For **2a** and **3a**, cis and trans forms, respectively, are predicted to be slightly preferred, whereas for **2b** the relative ordering depends on the density functional (cis preferred with BLYP, trans with B3LYP). In view of the small energy differences involved, definite conclusions concerning the stereochemistry in aqueous solution are difficult. For **2** and **3**, complex equilibria not only between four- and five-coordinated forms, but also between cis and trans isomers are to be expected.

Accurate computation of binding energies between dicationic uranyl hydrate **5** and chloride anions in aqueous solution is a difficult task for simple continuum models, because the huge differential hydration energies of reactants and products cannot always be fully described by screening effects in a dielectric. Even for a constant coordination number of five (cf. eq 4), notable driving forces are computed for formation of all complexes containing up to three or even four chlorides (Table 2). As just discussed, water dissociation from five-coordinate chloro complexes is predicted to be favorable with this approach when two or more chlorides are bound (Table 3). Allowing for such water elimination under concomitant formation of four-coordinate species would thus further increase the computed driving forces for binding of two or more halides. These PCM results are in contrast to experiment, where only the monochloro complex has a small negative free energy of formation, whereas all others are expected to be essentially unbound[3] and can only be populated at high or very high chloride concentrations. It would be interesting to see if static computations with explicit

inclusion of the second hydration sphere, i.e., by optimizing correspondingly microsolvated complexes,[55] could improve the computed binding energies in this case.

Instead of using such an elaborate, static model, we have included the full dynamics of the liquid. Indeed, the low affinity for uranyl and chloride in water is well reproduced qualitatively with constrained CPMD simulations and thermodynamic integration (Figure 2 and eq 6), but quantitatively the free energy of chloride binding is underestimated with this approach, probably due to shortcomings in the density functional employed, BLYP. Searching for other functionals that would allow for a better description of thermodynamic properties of the solutes without compromising the dynamic properties of the solvent could be rewarding.

At this point it should be noted that the occurrence of the tetrachloride **4** in aqueous solution is not established beyond doubt. It is likely that stabilization by gegenions,[56] as in the solid state, is necessary to prevent chloride dissociation. Only at the very high chloride concentration of a Dowex anion-exchange resin could some EXAFS-based evidence for its existence in aqueous solution be obtained.[4] Certainly, **4** is expected to be unstable in pure water, as well as in pristine form in the gas phase, where a notable driving force for dissociation of one chloride under formation of the coordinatively unsaturated $[UO_2Cl_3]^-$ had been computed at the B3LYP/LANL/6-31+G(d) level.[15b] Apparently such decomposition processes happen on a longer time scale than those of our first-principle MD simulations, where pristine and aqueous **4** is indicated to be metastable.

In summary, modeling the speciation of uranyl chloro complexes in aqueous solution is difficult terrain for density functional theory because of the small free-energy differences between the various species. Accurate description of solvation effects is crucial but appears difficult for simple continuum models in these systems. A CPMD-based approach treating the whole solution as a dynamic ensemble turns out to be a promising alternative. Geometrical parameters obtained with this dynamic approach and with static PCM optimizations are remarkably compatible with each other and can be used, in conjunction with EXAFS-derived bond distances, to assign total coordination numbers of five and four to aqueous uranyl monochloride and trichloride, respectively.

**Acknowledgment.** M.B. wishes to thank W. Thiel, the MPI für Kohlenforschung, and the Deutsche Forschungsgemeinschaft for support. A generous allotment of CPU time on an IBM p690 "Regatta" cluster at Rechenzentrum Garching is gratefully acknowledged. N.S. and G.W. thank CNRS−IDRIS, GDR PARIS, and University Louis Pasteur for support. We appreciate additional support in the framework of a German-French exchange program (DAAD/PROCOPE).

**Supporting Information Available:** LANL/BLYP-optimized coordinates for **1**−**5**, energies, structures, and Cartesian coordinates. This material is available free of charge via the Internet at http://pubs.acs.org.

## References and Notes

(1) McKibben, J. M. *Radiochim. Acta* **1984**, *36*, 3−15.

(2) Paiva, A. P.; Malik, P. *J. Radioanal. Nucl. Chem.* **2004**, *261*, 485−496.

(3) Extrapolated to standard conditions, a value of $\log_{10}\beta_1^0 = 0.17 \pm 0.02$ has been recommended for the equilibrium constant in the aqueous system $UO_2^{2+} + Cl^- \rightleftharpoons UO_2Cl^+$; the corresponding $\log_{10}\beta_2^0$ value is $-1.1 \pm 0.02$. See (a) Grenthe, I.; Fuger, J.; Konings, R. J. M.; Lemire, R. J.; Muller, A. B.; Nguyen-trung, C.; Wanner, H. *Chemical Thermodynamics Vol. 1: Chemical Thermodynamics of Uranium*; Wanner, H.; Forest I., Eds.; Elsevier: Amsterdam, 1992. (b) Guillaumont, R.; Fanghanel, T.; Fuger, J.; Grenthe, I.; Neck, V.; Palmer, D. A.; Rand, M. H. *Chemical Thermodynamics Vol. 5: Update on the Chemical Thermodynamics of Uranium, Neptunium, Plutonium, Americium, and Technetium*; Mompean, F. J.; Illemassene, M.; Domenech-Orti, C.; Ben Sais, K. OECD Nuclear Energy Agency, Eds.; Elsevier: Amsterdam, 2003. (c) See also: Grenthe, I.; Plyasunov, A. V.; Spahui, K. In *Modelling in Aquatic Chemistry*; Grenthe, I.; Puigdomenech, Eds.; OECD Publications, Nuclear Energy Agency: Paris, 1997; Chapter IX, pp 325−426 (www.nea.fr/dbtdb/pubs/Modelling_Book_TOC.htm).

(4) Allen, P. G.; Bucher, J. J.; Shuh, D. K.; Edelstein, N. M.; Reich, T. *Inorg. Chem.* **1997**, *36*, 4676−4683.

(5) Hennig, C.; Tutschku, J.; Rossberg, A.; Bernhard, G.; Scheinost, A. C. *Inorg. Chem.* **2005**, *44*, 6655−6661.

(6) The $[UO_2Cl_4]^{2-}$ ion is part of numerous single crystals characterized by X-ray crystallography; some representative examples are given in (a) di Spio, L.; Tondello, E.; Pellizzi, G.; Ingletto, G.; Montenero, A. *Cryst. Struct. Commun.* **1974**, *3*, 297 ($NMe4^+$ couterion). (b) Evans, D. J.; Junk, P. C.; Smith, M. K. *New J. Chem.* **2002**, *26*, 1043 (with a quaternary aza-crown ether and two crystal waters). (c) Rogers, R. D.; Bond, A. H. Hipple, W. G. *J. Crystallogr. Spectrosc. Res.* **1990**, *20*, 611 {$[Ca(15\text{-crown-}5)(H_2O)_3]^{2+}$ counterion}. According to a neutron-diffraction study, solid $UO_2Cl_2{\cdot}H_2O$ contains a pentagonal coordination environment consisting of four chloro and one water ligand about uranyl, but this involves chlorides that are bridging two uranyl moieties; see: (d) Taylor, J. C.; Wilson, P. W. *Acta Crystallogr., Sect. B: Struct. Crystallogr. Cryst. Chem.* **1974**, *30*, 169−175.

(7) For some selected reviews, see: (a) Denning, R. G. *J. Phys. Chem. A* **2007**, *111*, 4125−4143. (b) Vallet, V.; Macak, P.; Wahlgren, U.; Grenthe, I. *Theor. Chem. Acc.* **2006**, *115*, 145−160. (c) Szabó, Z.; Toraishi, T.; Vallet, V.; Grenthe, I. *Coord. Chem. Rev.* **2006**, *250*, 784−815. (d) Kaltsoyannis, N. *Chem. Soc. Rev.* **2003**, *32*, 9−16.

(8) For classical molecular-mechanical MD, see for example: (a) Guilbaud, P.; Wipff, G. *J. Mol. Struct. (THEOCHEM)* **1996**, *366*, 55−63. For more recent examples, see (b) Baaden, M.; Schurhammer, R.; Wipff, G. *J. Phys. Chem. B* **2002**, *106*, 434−441. (c) Chaumont, A.; Engler, E.; Wipff, G. *Inorg. Chem.* **2003**, *42*, 5348−5356. (d) Chaumont, A.; Wipff, G. *Chem. Eur. J.* **2004**, *10*, 3919−3930. (e) Galand, N.; Wipff, G. *J. Phys. Chem. B* **2005**, *109*, 277−287.

(9) Infante, I.; Visscher, L. *J. Comput. Chem.* **2003**, *25*, 386−392.

(10) (a) Bühl, M.; Diss, R.; Wipff, G. *J. Am. Chem. Soc.* **2005**, *127*, 13506−13507. (b) Bühl, M.; Kabrede, H.; Diss, R.; Wipff, G. *J. Am. Chem. Soc.* **2006**, *128*, 6357−6368.(c) Bühl, M.; Diss, R.; Wipff, G. *Inorg. Chem. 46* (13), 5196−5206.

(11) Bühl, M.; Kabrede, H. *Inorg. Chem.* **2006**, *45*, 3834−3836.

(12) Bühl, M.; Kabrede, H. *Chem. Phys. Chem.* **2006**, *7*, 2290−2293.

(13) Bühl, M.; Golubnychiy, V. *Inorg. Chem.* **2007**, *46*, 8129−8131.

(14) See for example: (a) Pierloot, K.; van Besien, E.; van Lenthe, E. J. *J. Chem. Phys.* **2007**, *126*, 194311. (b) Matsika, S.; Pitzer, R. M. *J. Phys. Chem. A* **2001**, *105*, 637−645.

(15) (a) Kovacs, A.; Konings, R. J. M. *J. Mol. Struct. (THEOCHEM)* **2004**, *684*, 35−42. (b) Chaumont, A.; Wipff, G. *Inorg. Chem.* **2004**, *43*, 5891−5901. (c) Clavaguera-Sarrio, C.; Hoyau, S.; Ismail, N.; Marsden, C. J. *J. Phys. Chem. A* **2003**, *107*, 4515−4525.

(16) van Besien, E.; Pierloot, K.; Gorller-Walrand. *Phys. Chem. Chem. Phys.* **2006**, *8*, 4311−4319.

(17) (a) Becke, A. D. *Phys. Rev. A* **1988**, *38*, 3098−3100. (b) Lee, C.; Yang, W.; Parr, R. G. *Phys. Rev. B* **1988**, *37*, 785−789.

(18) (a) Perdew, J. P. *Phys. Rev. B* **1986**, *33*, 8822−8824. (b) Perdew, J. P. *Phys. Rev. B* **1986**, *34*, 7406.

(19) Becke, A. D. *J. Chem. Phys.* **1993**, *98*, 5648−5642.

(20) Ortiz, J. V.; Hay, P. J.; Martin, R. L. *J. Am. Chem. Soc.* **1992**, *114*, 2736−2737, and references cited therein.

(21) As implemented in G 03: (a) Barone, V.; Cossi, M.; Tomasi, J. *J. Comput. Chem.* **1998**, *19*, 404−417. (b) Cossi, M.; Scalmani, G.; Rega, N.; Barone, V. *J. Chem. Phys.* **2002**, *117*, 43−54. (c) Cossi, M.; Crescenzi, O. *J. Chem. Phys.* **2003**, *19*, 8863−8872.

(22) Küchle, W.; Dolg, M.; Stoll, H.; Preuss, H. *J. Chem. Phys.* **1994**, *100*, 7535.

(23) (a) Krishnan, R.; Binkley, J. S.; Seeger, R.; Pople, J. A. *J. Chem. Phys.* **1980**, *72*, 650−654. (b) Clark, T.; Chandrasekhar, J.; Spitznagel, G. W.; Schleyer, P. v. R. *J. Comput. Chem.* **1983**, *4*, 294−301.

(24) Boys, S. F.; Bernardi, F. *Mol. Phys.* **1970**, *19*, 553−566.

(25) Frisch, M. J.; Trucks, G. W.; Schlegel, H. B.; Scuseria, G. E.; Robb, M. A.; Cheeseman, J. R.; Montgomery, J. A., Jr.; Vreven, T.; Kudin, K. N.; Burant, J. C.; Millam, J. M.; Iyengar, S. S.; Tomasi, J.; Barone, V.; Mennucci, B.; Cossi, M.; Scalmani, G.; Rega, N.; Petersson, G. A.; Nakatsuji, H.; Hada, M.; Ehara, M.; Toyota, K.; Fukuda, R.; Hasegawa, J.; Ishida, M.; Nakajima, T.; Honda, Y.; Kitao, O.; Nakai, H.; Klene, M.; Li, X.; Knox, J. E.; Hratchian, H. P.; Cross, J. B.; Adamo, C.; Jaramillo, J.; Gomperts, R.; Stratmann, R. E.; Yazyev, O.; Austin, A. J.; Cammi, R.; Pomelli, C.; Ochterski, J. W.; Ayala, P. Y.; Morokuma, K.; Voth, G. A.;

Salvador, P.; Dannenberg, J. J.; Zakrzewski, V. G.; Dapprich, S.; Daniels, A. D.; Strain, M. C.; Farkas, O.; Malick, D. K.; Rabuck, A. D.; Raghavachari, K.; Foresman, J. B.; Ortiz, J. V.; Cui, Q.; Baboul, A. G.; Clifford, S.; Cioslowski, J.; Stefanov, B. B.; Liu, G.; Liashenko, A.; Piskorz, P.; Komaromi, I.; Martin, R. L.; Fox, D. J.; Keith, T.; Al-Laham, M. A.; Peng, C. Y.; Nanayakkara, A.; Challacombe, M.; Gill, P. M. W.; Johnson, B.; Chen, W.; Wong, M. W.; Gonzalez, C.; Pople, J. A. Gaussian 03, Gaussian, Inc., Pittsburgh, PA, 2003.

(26) CPMD Version 3.9.2, Copyright IBM Corp., 1990−2006, Copyright MPI für Festkörperforschung Stuttgart, 1997−2001.

(27) Troullier, N.; Martins, J. L. *Phys. Rev. B* **1991**, *43*, 1993−2006.

(28) Kleinman, L.; Bylander, D. M. *Phys. Rev. Lett.* **1982**, *48*, 1425−1428.

(29) Car, R.; Parrinello, M. *Phys. Rev. Lett*. **1985**, *55*, 2471−2474.

(30) It is difficult to ensure full equilibration after such a short time. In some cases, in particular for **4**, the simulations may just be metastable, and much longer simulation times might be needed to reach the true ground states. However, all observable parameters discussed, i.e., bond distances or mean constraint forces, were reasonably well converged within the duration of the simulations, without showing noticeable drifts.

(31) Marx, D.; Hutter, J.; Parrinello, M. *Chem. Phys. Lett*. **1995**, *241*, 457−462.

(32) Sprik, M.; Ciccotti, G. *J. Chem. Phys*. **1998**, *109*, 7737−7744, and references cited therein.

(33) Some of the gas-phase minima showed more and larger imaginary frequencies upon reoptimization in the continuum (exceeding 200*i* $cm^{-1}$); in these cases lower-lying stationary points were located in the continuum (true minima in most cases), which are labeled (PCM) in the Supporting Information.

(34) The initial CPMD/BLYP simulations in the Parrinello group have afforded good descriptions of liquid water, see for instance: (a) Sprik, M.; Hutter, J.; Parrinello, M. *J. Chem. Phys*. **1996**, *105*, 1142−1152, although potential shortcomings of this functional are now better appreciated; see (b) VandeVondele, J.; Mohamed, F.; Krack, M.; Hutter, J.; Sprik, M.; Parrinello, M. *J. Chem. Phys.* **2005**, *122*, 014515, and references cited therein.

(35) Shamov, G. A.; Schreckenbach, G.; Vo, T. N. *Chem. Eur. J*. **2007**, *13*, 4932−4947.

(36) Occasionally, pure GGAs such as the BP86 functional also perform satisfactorily in computations of thermodynamic properties of the uranyl ion, see for example: Moskaleva, L. V.; Matveev, A. V.; Krüger, S.; Rösch, N. *Chem. Eur. J.* **2006**, *12*, 629−634.

(37) (a) Bühl, M.; Kabrede, H. *J. Chem. Theory Comput*. **2006**, *2*, 1282−1290. (b) Waller, M. P.; Braun, H.; Hojdis, N.; Bühl, M. *J. Chem. Theor. Comput*. **2007**, *3*, 2234−2242.

(38) The shorter B3LYP values appear to be more consistent with experiment, but we do not dismiss the BLYP level based on this finding, because the errors in the geometrical parameters are fairly systematic throughout. Thus, *relative* energies should be affected only to a small extent. Even the error in terms of *absolute* energies is indicated to be quite small: According to single-point energy computations at a sophisticated multireference ab initio level for a uranyl hydrate complex, a BLYP/SCRF optimized geometry (despite its elongated U═O distances) is only 0.9 kcal/mol higher in energy than the corresponding B3LYP/SCRF geometry (which shows more accurate U═O bond lengths); see Table 5 in ref 51b. Unfortunately, the use of hybrid functionals such as B3LYP is prohibitively expensive with CPMD.

(39) Shamov, G. A.; Schreckenbach, G. *J. Phys. Chem. A* **2005**, *109*, 10961−10974.

(40) For the more strongly bound uranyl fluoride complexes, B3LYP-optimized U−F bond lengths were found to be in good accord with EXAFS-derived values: Vallet, V.; Wahlgren, U.; Schimmelpfennig, B.; Moll, H.; Szabo, Z.; Grenthe, I. *Inorg. Chem*. **2001**, *40*, 3516−3525.

(41) At the SDD+//LANL levels, the Counterpoise-derived estimates for the BSSE of the equatorial bond types are remarkably similar for five-coordinate complexes **1a**−**5**. For **1a**, these corrections amount to 0.87 kcal/mol and 1.98 kcal/mol for U−Cl and U−O bonds, respectively, at the BLYP/SDD(+)//BLYP/SDD level [0.81 and 1.98 kcal/mol, respectively, at B3LYP/SDD(+)//SDD]. These values have been used to evaluate the $\Delta E^{CP}$ entries in Table 2 and 3.

(42) Vallet, V.; Wahlgren, U.; Grenthe, I. *J. Am. Chem. Soc*. **2003**, *125*, 14941−14950.

(43) MD simulations performed at constant volume yield Helmholtz free energies, $\Delta A$. In practice, for condensed phases these should be very close to the Gibbs free energies, $\Delta G$, obtained at constant pressure, because volume changes in a liquid are usually very small.

(44) This uncertainty refers to the numerical precision of the PTI technique. The absolute uncertainty due to the accuracy of the underlying quantum-chemical methodology (density functional, pseudopotential, basis set) is, arguably, considerably higher and is at least ±2.5 kcal/mol, judged from the errors in computed kinetic and thermodynamic parameters relative to experiment (refs 11−13).

(45) See for instance: Morel, F. M. M.; Hering, J. G. *Principles and Applications of Aquatic Chemistry*; John Wiley & Sons: New York, 1993; p 399, where a simple expression from statistical considerations of electrostatic interactions between ions in a dielectric continuum was used for this estimate.

(46) In principle, the relative free energy between start and end point of a thermodynamic integration does not depend on the path in between. We are not attempting to model the mechanism of the actual displacement process, which may well (in analogy to water exchange, see ref 11) follow an associative rather than the dissociative path implicitly assumed in the present paper.

(47) Following the argument in Martin, R. L.; Hay, P. J.; Pratt, L. R. *J. Phys. Chem. A* **1998**, *102*, 3565−3573, where this simple procedure has been proposed as adjustment for the concentration of water molecules in the liquid, and where the necessary value for the pressure has been derived from the experimental density of liquid water. Even though less well defined for the other occurring species besides water, we used the same pressure correction throughout (implying standard reference states of infinitely diluted aqueous solutions). In the implementation in *Gaussian 03*, the change in absolute free energy on going at 298.15 K from a pressure of 1 atm to 1354 atm amounts to +4.3 kcal/mol per particle, irrespective of the particle and the level of theory. This correction affects only the translational part of the entropy and, thus, applies only to reactions where the particle number changes, such as eq 7 and not to those where it is constant, such as eqs 4 and 2a.

(48) See for example: (a) Burns, P. C.; Ewing, R. C.; Hawthorne, F. C. *Canad. Mineral*. **1997**, *35*, 1551−1570. (b) Burns, J. H. Structural Chemistry. In *The Chemistry of the Actinide Elements*, 2nd ed.; Katz, J. J.; Seaborg, G. T.; Morss, L. R., Eds.; Chapman and Hall: New York, 1986; Vol. 2, Chapt. 20, pp 1417−1479.

(49) With chelating ligands with small bite angle, such as nitrate, six-coordination is also quite common; see for example: (a) Dalley, N. K.; Mueller, M. H.; Simonsen, S. H. *Inorg. Chem*. **1971**, *10*, 323−328. (b) Villiers, C.; Thuery, P.; Ephritikhine, M. *Polyhedron* **2004**, *23*, 1613−1618. (c) Crawford, M.-J.; Mayer, P. *Inorg. Chem*. **2005**, *44*, 8481−8485.

(50) In contrast, four fluoro ligands can accommodate a fifth donor, as exemplified in the $[UO_2F_4(H_2O)]^{2-}$ ion; see for example: Vallet, V.; Wahlgren, U.; Schimmelpfennig, B.; Moll, H.; Szabo, Z.; Grenthe, I. *Inorg. Chem.* **2001**, *40*, 3516−3525.

(51) See for instance: (a) Rotzinger, F. R. *J. Phys. Chem. B* **2005**, *109*, 1510−1527; (b) Rotzinger, F. R. *Chem. Eur. J.* **2007**, *13*, 800−811.

(52) For instance, the free-energy difference between uranyl penta- and hexahydrate, decisive for the activation barrier for water exchange in the pentahydrate, is underestimated by ca. 2 kcal/mol with our CPMD/PTI methodology (ref 11).

(53) A referee has suggested to look at the uranyl stretching frequencies as potential probe for the coordination number. For **1a** and **1b**, however, very similar $UO_2$ stretching vibrations are obtained in the continuum (e.g. $\omega_{asym}$ = 894 and 891 $cm^{-1}$ for **1a** and **1b**, respectively, at BLYP/SDD/PCM), suggesting that this property is probably a poor indicator for the coordination number in uranyl chloride complexes.

(54) Haller, L. J. L.; Kaltsoyannis, N.; Sarsfield, M. J.; May, I.; Cornet, S. M.; Redmond, M. P.; Helliwell, M. *Inorg. Chem.* **2007**, *46*, 4868−4875.

(55) See for instance: Siboulet, B.; Marsden, C. J.; Vitorge, P. *Chem. Phys*. **2006**, *326*, 289−296.

(56) While it would be desirable to include the counterions in the CPMD simulations, we have not done so, because those present in the experiments (typically alkali metal cations) are usually well hydrated, forming solvent-separated, rather than contact ion pairs. Realistic computational modeling of the real solutions would require much larger boxes and, in particular, much larger simulation times, as the relative diffusion of hydrated ions happens on a longer time scale. It is well possible that even such distant counterions could exert noticeable effects on the properties under scrutiny, but most likely this would just fine-tune the latter, not radically alter them.